PAPER • OPEN ACCESS

Nonabelian Ginzburg–Landau theory for ferroelectrics

View the article online for updates and enhancements.

Nonabelian Ginzburg–Landau theory for ferroelectrics

You-Quan Li[1,2,6,*] , **Pei Wang**[3,*], **Hua Zhang**[4], **Hong Zhang**[2] **and Li-Bin Fu**[5]

[1] Chern Institute of Mathematics, Nankai University, Weijin Road 94, Tianjin 300071, People's Republic of China
[2] School of Physics, Zhejiang University, Hangzhou 310027, People's Republic of China
[3] Department of Physics, Zhejiang Normal University, Jinhua 321004, People's Republic of China
[4] Center for Advanced Material Diagnostic Technology, Shenzhen Technology University, Shenzhen 518118, People's Republic of China
[5] Graduate School of China Academy of Engineering Physics, Beijing 100193, People's Republic of China
[6] Collaborative Innovation Center of Advanced Microstructure, Nanjing University, Nanjing 210008, People's Republic of China

E-mail: yqli@zju.edu.cn and wangpei@zjnu.cn

CrossMark

Abstract

The Ginzburg–Landau theory, which was introduced to phenomenologically describe the destruction of superconductivity by a magnetic field at the beginning, has brought up much more knowledge beyond the original one as a mean-field theory of thermodynamics states. There the complex order parameter plays an important role. Here we propose a macroscopic theory to describe the features of ferroelectrics by a two-component complex order parameter coupled to nonabelian gauge potentials that provide more freedom to reflect interplays between different measurables. Within this theoretical framework, some recently discovered empirical static and time-independent phenomena, such as vortex, anti-vortex, spiral orders can be obtained as solutions for different gauge potentials. It is expected to bring in a new angle of view with more elucidation than the traditional one that takes the polarization as order parameter.

Keywords: ferroelectrics, Gingzburg–Landau theory, electric polarization, spiral order, vortex order, free energy, nonableian gauge field

(Some figures may appear in colour only in the online journal)

1. Introduction

The ferroelectric material is an insulating system with spontaneous polarization [1–4]. The polarity used to dominate the field of ferroelectricity at the beginning [5, 6], however, its combination with more exotic features like vortex, skyrmions, and domain walls [7–9] has now entered the stage and substantially expanded the field of applications [10–12]. Especially, domain walls and their functionalities, which have long been ignored, are speculated to be valuable tools for memoristic devices [12, 13] and be interesting for neuromorphic applications. In order to construct new types of multifunctional devices, much of the future progress courts on the delivery of improved chemistries and microstructures [14, 15], and on bridging the understanding of current atomistic and phenomenological descriptions.

---

* Authors to whom any correspondence should be addressed.

The influence of electric and magnetic fields on the electric polar topological structures [7–10] has been aware both in microscopic theories and experiments. Ab-initio calculation revealed that a cylindrical BaTiO$_3$ nanowire embedded in a SrTiO$_3$ matrix exhibits a Bloch skymion structure [16]. The material GaV$_4$S$_8$ has both the ferroelectric and ferromagnetic orders below 44K, while the excess polarization may show cycloidal or skymion structure, depending on the external magnetic field and temperature. The experimental observation is explained by the spin-driven mechanism [17]. The BiFeO$_3$/GdScO$_3$/BiFeO$_3$ sandwich structure on TbScO$_3$ substrate displays both the flux-closure and vortices topological structure [18]. The vortex domain walls were discovered in the PbTiO$_3$/SrTiO$_3$ superlattice which was explained as the boundary effect [11]. Not only vortices exist in PbTiO$_3$ layer but also anti-vortices have been found in SrTiO$_3$ [10, 11].

Phenomenological formalism often provides important qualitative and reasonable quantitative results with an appropriate choice of the coefficients. Conventionally, the macroscopic modeling of ferroelectric properties refers to the Landau–Ginzburg–Devonshire theory [19–22]. In the conventional literature, the interplay between polarization and magnetization is described by introducing terms of their product in the free energy [23], while the interplay between structural, ferroelectric and magnetic defects is described by using an expansion of the free energy in powers of the corresponding order paramers and their gradients [24]. The traditional approach that directly takes the polarization as order parameter captures less intrinsic characteristics because quantum coherence that is related to phase of complex order parameter was missing. Note that one is able to go beyond the standard thermodynamics by introducing a complex order parameter in the Ginzburg–Landau (GL) phenomenological theory for superconductors [25]. Meanwhile, various exotic spin orders [26, 27], such as conical spiral, in-plane spiral, helical, as well as the ferromagnetic orders can be unified as different solutions of the Landau–Lifshitz equation with different nonabelian gauge potentials [28]. There the nonabelian gauge potential plays the role of connection that defines a nontrivial parallel transport resulting versatile scene frames. The comprehensive role that nonabelian field played also includes Rashba spin–orbit coupling in certain semiconductor [29] and in cold atoms [30, 31]. Thus, whether the Landau's U(1) order parameter used to describe superconductors can be developed further is an promising issue. It is thus worthwhile to set up a phenomenological theory that provides a unified description for electric polarization orders. Here we show that two-component order parameters give rise to a general macroscopic theory for ferroelectricity. The SU(2) gauge potentials associated with the two-component order parameter are matrix valued and characterized by twelve parameters. The interplay between the electric polarization and other variables is naturally reflected through the coupling between order parameters and gauge potentials. It is expected to bring in a new angle of view in phenomenological descriptions with more elucidation. Some empirical static and time-independent phenomena are featured through solutions of the theory.

2. Phenomenological theory with complex order parameters

The most essential concept in phenomenological description of dielectric media is the macroscopic electric polarization that was regarded [32] as electric dipole moment per unit volume. However, fallacies were encountered if it were defined by the dipole of either a macroscopic sample or a unit cell of crystalline lattice divided by the corresponding volume. To avoid this, in a modern theory [6, 33] of polarization (refers to the electric polarization hereafter for simplicity), the change in the polarization is shown to be related to a charge flow in the interior of the sample during an adiabatic process [5, 33, 34]. By introducing a local polarization vector $\boldsymbol{P} = \boldsymbol{P}(x, y, z)$ in a continuum model, Landau's symmetry-based formalism of phase transition [20] was applied to systems with spatially uniform polarization, which is called Landau–Devonshire theory [19]. It is further developed to nonuniform case [21] by taking account of the variations in the direction of the polarization [6]. Conventionally, the free energy density is written as

$$\mathcal{F}_{\text{LD}} = |\nabla \boldsymbol{P}|^2 - \boldsymbol{E} \cdot \boldsymbol{P} - \alpha |\boldsymbol{P}|^2 + \beta |\boldsymbol{P}|^4 \qquad (1)$$

where $\boldsymbol{E}$ is the applied external electric field, and ∇ denotes spatial derivative. Here the parameters α and β depend on temperature and pressure.

Clearly, it is lack of some essential information in the free energy (1) where the polarization vector $\boldsymbol{P}$ itself is regarded as an order parameter. The polarization has nothing to do with the periodic charge distribution of the polarized crystal because, quantum mechanically, the charge distribution is related to the modulus while the polarization is the property of the phase of the electronic wavefunction [6]. Motivated by the complex order parameter for superconductors where the electromagnetic fields was naturally introduced via U(1) gauge transformation, here we consider multi-component complex order parameters for ferroelectrics. As its micro-mechanism involves the interplay between many degree of freedoms, such as spin, charge, orbital as well as lattice dynamics, the macroscopic theory in terms of multi-component order parameters is expected to reflect effects arising from their interplays automatically and present a unified phenomenological description.

2.1. On complex order parameters

We consider a two-component order parameter $\Psi^\dagger = (\psi_1^*, \psi_2^*)$ and the corresponding free energy density,

$$\mathcal{F} = \frac{1}{2}|(\nabla_i + \kappa \mathcal{A}_i)\Psi|^2 + \frac{\lambda^2}{2}\left(|\Psi|^2 - \eta^2\right)^2$$
$$+ i\Psi^\dagger A_0^a \tau^a \Psi - \frac{1}{4}\left(F_{\mu\nu}^a\right)^2 \qquad (2)$$

which is a multi-parameter generalization of Ginzburg–Landau theory. Here the covariant derivative $\nabla_i + \kappa \mathcal{A}_i$

($i = 1, 2, 3$) along the ith direction is defined by nonabelian gauge potentials:

$$\mathcal{A}_\mu = \sum_{a=1}^{3} A_\mu^a \tau^a, \quad (\mu = 0, 1, 2, 3)$$

that are valued in the Lie algebra of SU(2) group. Here τ^a ($a = 1, 2, 3$) refer to the matrix bases of that Lie algebra [35] satisfying $[\tau^a, \tau^b] = -\epsilon^{abc}\tau^c$ and hence $\mathcal{A}_\mu = -\mathcal{A}_\mu^\dagger$ is antihermitian and A_μ^a is a real number. Here superscript a, b, c labels the component in intrinsic space (i.e. Lie algebra space). These nonabelian gauge potentials define the field strength tensor [36],

$$F_{\mu\nu}^a = \partial_\mu A_\nu^a - \partial_\nu A_\mu^a - \kappa \, \epsilon^{abc} A_\mu^b A_\nu^c \quad (3)$$

where ε^{abc} is the three-dimensional Levi-Civita tensor and the Einstein abbreviation was adopted in the summation of repeated indices hereafter. Note that the nonlinear term of gauge potential in (3) is absent in abelian case. The last term in the free energy density (2) arises from such a strength tensor (3). The third term in equation (2) represents the contribution of the interaction between the polarization field and an external electric field, that implies $A_0^a \sim E_a$. For simplicity in expression, hereafter we choose the unit of the gauge potential so that the coupling strength $\kappa = 1$. In this paper, we mainly consider the spontaneous symmetry breaking term $U(|\Psi|) = \frac{1}{2}\lambda^2(|\Psi|^2 - \eta^2)^2$ in the free energy (2) at very low temperature. Higher order terms become not neglectable near the critical temperature. Here $\eta \neq 0$ for ferroelectric and λ is related to dielectric constant when $\eta = 0$.

The two-component complex order parameter Ψ defines a spatially dependent physical quantity $\boldsymbol{P} = (P_1, P_2, P_3)$, the polarization vector field, through the following formula

$$P_a = \Psi^\dagger \sigma^a \Psi \quad (4)$$

where σ^a is the conventional Pauli matrix that provides a realization of the generators of SU(2), i.e. $\tau^a = i\sigma^a/2$. This vector (4) is invariant under the U(1) gauge transformation. Clearly, the free energy (2) satisfies local SU(2) gauge invariance. Whereas, the expression (4) is not necessarily gauge invariant since the polarization vector $\boldsymbol{P}$ changes its direction if the coordinate frame rotates. The compatibility is guaranteed by the homomorphism between the SU(2) unitary transformation and SO(3) rotation.

The gauge potential that defines the covariant derivative can reflect the effects of electric, magnetic as well as certain intrinsic features arising from chemistries and microstructure of certain material. Conventionally, the ferroelectricity used to be described as the result of relative shifts of negative and positive ions that induce surface charges, the concrete concepts of charges are not necessary in present formalism. Moreover, more intrinsic features can be reflected in terms of multicomponent order parameters. Let us analyze the internal symmetries hidden in the order parameters we introduced. Since the charge conjugation will transform the polarization vector

$\boldsymbol{P}$ into $-\boldsymbol{P}$, which corresponds to a $\pi/2$ rotation of the spinor Ψ, our order parameter transforms as

$$\begin{pmatrix} \psi_1 \\ \psi_2 \end{pmatrix} \rightarrow \begin{pmatrix} -\psi_2^* \\ \psi_1^* \end{pmatrix}$$

under charge conjugation. Such transformation can be represented via operator $-i\sigma^2\hat{C}$ with $\hat{C}$ standing for complex conjugation and σ^2 the y-component Pauli matrix. One can perceive that the order parameters here define a charge complex plane that characterizes more implications than the naive picture of density of positive or negative charge distributions. The independence of the choice of bases of the complex plane naturally implies the existence of SU(2) gauge potential.

2.2. Implications of gauge potentials

We turn to investigate what is naturally implied in the SU(2) gauge potentials. It will be helpful to observe the force that a moving electric dipole undergoes in electric and magnetic fields, $\boldsymbol{E}$ and $\boldsymbol{B}$. A dipole $\boldsymbol{d} = (d^1, d^2, d^3)$ at $\boldsymbol{r}$ can be regarded as a positive charge $+q$ at $\boldsymbol{r} + \boldsymbol{\ell}/2$ and a negative charge $-q$ at $\boldsymbol{r} - \boldsymbol{\ell}/2$ such that $\boldsymbol{d} = \lim_{\ell \to 0} q\boldsymbol{\ell}$. Let $\boldsymbol{v}$ denote the velocity of the center of the dipole, the velocities of the positive and the negative charges are $\boldsymbol{v} + \dot{\boldsymbol{\ell}}/2$ and $\boldsymbol{v} - \dot{\boldsymbol{\ell}}/2$, respectively. Here the overhead dot denotes the time derivative. Expanding the Lorentz forces acting on these two charges, neglecting the higher orders (in the limit of $\ell \to 0$) and noticing that a moving dipole will experience a torque [37] in electromagnetic fields, $\dot{\boldsymbol{d}} = \boldsymbol{d} \times (\boldsymbol{E} + \frac{\boldsymbol{v}}{c} \times \boldsymbol{B})$, we obtain the total force, $\boldsymbol{f}$, that the dipole feels

$$\boldsymbol{f} = (\boldsymbol{d} \cdot \nabla)\boldsymbol{E} + \frac{\boldsymbol{v}}{c} \times [\nabla \times (\boldsymbol{B} \times \boldsymbol{d})]$$
$$+ \boldsymbol{B} \times \left[\left(\boldsymbol{E} + \frac{\boldsymbol{v}}{c} \times \boldsymbol{B}\right) \times \boldsymbol{d} \right]. \quad (5)$$

This exhibits that the force formula includes nonlinear terms of electromagnetic fields. Such an esoteric feature is naturally reflected in the two-component Ginzburg–Landau formalism with the SU(2) gauge field, in which the force formula is given by

$$f_i = J_\mu^a F^a{}_{\mu i} \quad (6)$$

and the nonabelian field strength tensor (3) contains quadratic terms bringing in nonlinear terms automatically. Here J_μ^a denotes the dipole four-current in space-time $x_\mu = (x_0, \boldsymbol{r})$, $x_0 = ct$. For a moving dipole, the temporal component J_0^a refers to the dipole moment d^a and the spatial component J_i^a to the dipole current $d^a v_i/c$.

The polarization field $\boldsymbol{P}$ describing a moving single dipole reads $\boldsymbol{P}(\boldsymbol{r}, t) = \boldsymbol{d}(t)\delta(\boldsymbol{r} - \tilde{\boldsymbol{r}}(t))$ with $\tilde{\boldsymbol{r}}(t)$ being its trajectory. Because the dipole can be regarded as a positive charge $+q$ at $\boldsymbol{r} + \boldsymbol{\ell}/2$ and a negative charge $-q$ at $\boldsymbol{r} - \boldsymbol{\ell}/2$, the electric current produced by those two charges gives rise to $\boldsymbol{j} = \lim_{\ell \to 0} q\dot{\boldsymbol{\ell}} = \dot{\boldsymbol{d}} = \boldsymbol{d} \times (\boldsymbol{E} + \frac{\boldsymbol{v}}{c} \times \boldsymbol{B})$. The interaction terms contributed by the first term and the third term in the free energy (2) are $J_\mu^a A_\mu^a$,

which is in agreement with the case of a moving dipole [37], $\boldsymbol{d} \cdot (\boldsymbol{E} + \frac{\boldsymbol{v}}{c} \times \boldsymbol{B})$. Then we perceive that the local fields A_0^a and A_i^a represent, respectively, E_a and $\epsilon_{aij}B_j$ for such a particular case at least.

Since in the Maxwell equation we have

$$\nabla \times \boldsymbol{B} - \frac{1}{c}\frac{\partial \boldsymbol{E}}{\partial t} = \frac{4\pi}{c}\boldsymbol{j} \qquad (7)$$

which is consistent with the following gauge condition for the SU(2) gauge potential

$$\partial^\mu A_\mu^a = -\frac{4\pi}{c}j^a \qquad (8)$$

where we adopted the conventional metric of Bjorken and Drell, $g_{\mu\nu} = \mathrm{diag}(1, -1, -1, -1)$. Clearly, the so-called Lorentz gauge $\partial^\mu A_\mu^a = 0$ corresponds to the case of vanishing current $\boldsymbol{j} = 0$. Note that, only A_0^a stands for electric field E_a while A_i^a can be more general than $\epsilon_{aij}B_j$, the aforementioned particular case. Actually there are additional six parameters in A_μ^a, namely,

$$\begin{aligned}
\vec{A}_x &= (g_1, b_3 - B_z, b_2 + B_y) \\
\vec{A}_y &= (b_3 + B_z, g_2, b_1 - B_x) \\
\vec{A}_z &= (b_2 - B_y, b_1 + B_x, g_3) \\
\vec{A}_0 &= (E_x, E_y, E_z)
\end{aligned} \qquad (9)$$

where B's and E's also obey the other three of Maxwell equations,

$$\begin{aligned}
\nabla \cdot \boldsymbol{B} &= 0, \\
\nabla \times \boldsymbol{E} + \frac{1}{c}\frac{\partial \boldsymbol{B}}{\partial t} &= 0, \\
\nabla \cdot \boldsymbol{E} &= 4\pi\rho
\end{aligned} \qquad (10)$$

where ρ includes contributions from both free and bound charges. In other words, the SU(2) gauge potentials expressed by equation (9) with constants b's and g's together with functions $\boldsymbol{B}(\boldsymbol{r})$ and $\boldsymbol{E}(\boldsymbol{r})$ fulfil the Lorentz gauge condition (8).

3. Some solutions of the theory

As applications of the above nonabelian GL formalism, let us investigate electric polarization in response to the SU(2) temporal and spatial components, successively, i.e. the case $\mathcal{A}_0 \neq 0$, $\mathcal{A}_i = 0$ and then the case $\mathcal{A}_0 = 0$, $\mathcal{A}_i \neq 0$.

3.1. Electric ferroelectrics

We have shown in the previous section that the effect of electric fields is characterized by the temporal component of SU(2) gauge potential $\mathcal{A}_0 = 2E_a\tau^a$. In this case $\mathcal{A}_0 \neq 0$, while $\mathcal{A}_i = 0$, the covariant derivatives reduce to the conventional derivatives in flat space and the free energy density then reads

$$\mathcal{F} = \frac{1}{2}|\nabla\Psi|^2 + \frac{\lambda^2}{2}(|\Psi|^2 - \eta^2)^2 - E_a\Psi^\dagger\sigma^a\Psi - 2(\nabla E_a)^2 \qquad (11)$$

in which the third term corresponds to $-\boldsymbol{E} \cdot \boldsymbol{P}$ in agreement with the electromagnetism theory. Let us consider some typical electric fields that can be easily produced in experiment. The simplest case is a uniform electric field which we will revisit later on. In order to observe the effect caused by the kinetic term in the free energy (11), we need consider nonuniform electric field. First example is the electric field produced by a charged line perpendicular to the x–y plane

$$\boldsymbol{E} = \frac{\gamma}{x^2 + y^2}(x\boldsymbol{e}_x + y\boldsymbol{e}_y) \qquad (12)$$

where γ is a constant and $\boldsymbol{e}_x$ and $\boldsymbol{e}_y$ denote the unit vector along x- and y-axis respectively. This is the case $\vec{A}_i = 0$ and $\vec{A}_0 = \gamma/(x^2 + y^2)(x, y, 0)$. By minimizing the free energy (11), we find the polarization far away from the origin to be

$$\boldsymbol{P} = (\pm\eta^2\cos\theta, \pm\eta^2\sin\theta, 0)$$

where the plus and minus sign corresponds to $\gamma > 0$ and $\gamma < 0$ respectively. Here θ denotes the azimuthal angle.

Another example is a curling electric field produced by applying alternative electric current in a thin solenoid placed in perpendicular to the x–y plane,

$$\boldsymbol{E} = \frac{\gamma}{x^2 + y^2}(-y\boldsymbol{e}_x + x\boldsymbol{e}_y) \qquad (13)$$

which means $\vec{A}_i = 0$ and $\vec{A}_0 = \gamma/(x^2 + y^2)(-y, x, 0)$. The polarization far away from the origin is solved as

$$\boldsymbol{P} = (\eta^2\cos(\theta \pm \pi/2), \eta^2\sin(\theta \pm \pi/2), 0).$$

Again, here the plus or minus sign takes for $\gamma > 0$ or $\gamma < 0$, respectively. Figure 1 illustrates the aforementioned two solutions for the distribution of polarization in a round sample. The detailed derivations are given in the appendix.

3.2. Magnetic ferroelectrics

As we shown in previous section, the magnetic field is related to the spatial component $\mathcal{A}_i$ of the gauge potential. This is the case of $\mathcal{A}_0 = 0$ but $\mathcal{A}_i \neq 0$, thus the free energy density is expressed as

$$\mathcal{F} = \frac{1}{2}|(\nabla_i + A_i^a\tau^a)\Psi|^2 + \frac{\lambda^2}{2}(|\Psi|^2 - \eta^2)^2 - \frac{1}{4}(F^a{}_{\mu\nu})^2. \qquad (14)$$

Let us consider several typical magnetic fields. One is the magnetic field produced by a pairs of opposed Helmholz coils which was also applied to trap cold atoms.

$$\boldsymbol{B} = \gamma(x\boldsymbol{e}_x + y\boldsymbol{e}_y - 2z\boldsymbol{e}_z).$$

The magnitude of such field is given by $B = \gamma(x^2 + y^2 + 4z^2)^{1/2}$. The corresponding SU(2) gauge potentials are $\vec{A}_x = \gamma(0, 2z, y)$, $\vec{A}_y = \gamma(-2z, 0, -x)$, $\vec{A}_z = \gamma(-y, x, 0)$, and $\vec{A}_0 = 0$. Considering a square-shaped sample in the x–y plane, we numerically solve the order parameter $\Psi(x, y)$ by minimizing
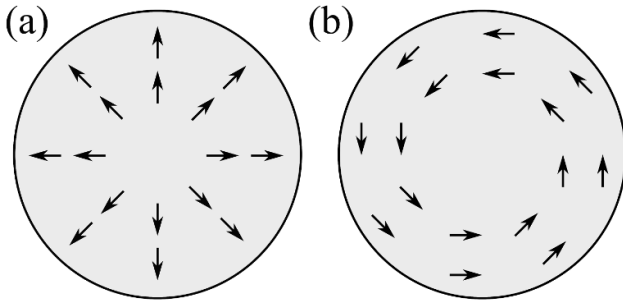
Figure 1. Schematic illustration of analytical solutions far away from the origin in response to (a) $\boldsymbol{E} = \gamma(x/(x^2+y^2), y/(x^2+y^2))$ and (b) $\boldsymbol{E} = \gamma(-y/(x^2+y^2), x/(x^2+y^2))$ where the arrows indicate the directions of $\boldsymbol{P}$. The helicity of the latter vortex is one while that of the former is zero.

the free energy (see the appendix for details). Figure 2 exhibits the resulting distribution of polarization $\boldsymbol{P}$, in which the x- and y-components are plotted out while the z-component is approximately zero everywhere. We can see that the configuration of polarization field forms an anti-vortex crystal where one of them is marked by red dash-line circle. The polar anti-vortex has been experimentally created in PbTiO$_3$/SrTiO3 superlattice recently [11]. Conceptionally, vorticity is a quantity that characterizes topology properties of any vector field around its singularity point. If the direction of the vector changes and accumulates precisely a 2π variation after observing it along a directed close curve around the singularity point, it is named as a vortex. Instead, if it accumulates in the opposite direction, saying -2π, it is then named as anti-vortex. Vortices are further specified by another quantity called helicity which is evaluated by the line-integral of the vector field along a directed close curve. It can be either negative or positive depending on its curling clockwise or anti-clockwise; and is zero in case of no curling. For anti-vortex, however, its helicity is always zero.

The second one is a in-plane magnetic field

$$\boldsymbol{B} = \gamma(x\boldsymbol{e}_x - y\boldsymbol{e}_y)$$

with magnitude $B = \gamma(x^2+y^2)^{1/2}$. The corresponding SU(2) gauge potentials read $\vec{A}_x = \gamma(0,0,-y)$, $\vec{A}_y = \gamma(0,0,-x)$, $\vec{A}_z = \gamma(y,x,0)$, and $\vec{A}_0 = 0$. We numerically solve the distribution of $\boldsymbol{P}$ and plot the result in figure 3. Again, P_z is found to be approximately zero everywhere. One can see the formation of strip-like pattern, namely, there are four arc-type strips centering at four corners of the sample, respectively. In the figure, two red dash-line arrows indicate the track of spiral orders: along top one the $\boldsymbol{P}$ rotates clockwise while along the bottom one it rotates anti-clockwise.

Clearly, the curl of the above two magnetic fields vanishes. An example of magnetic field with non-vanishing curl reads,

$$\boldsymbol{B} = \gamma(-y\boldsymbol{e}_x + x\boldsymbol{e}_y)$$

which satisfies the gauge condition (8) with $j^3/c = \gamma/2\pi$. The corresponding SU(2) gauge potentials are expressed
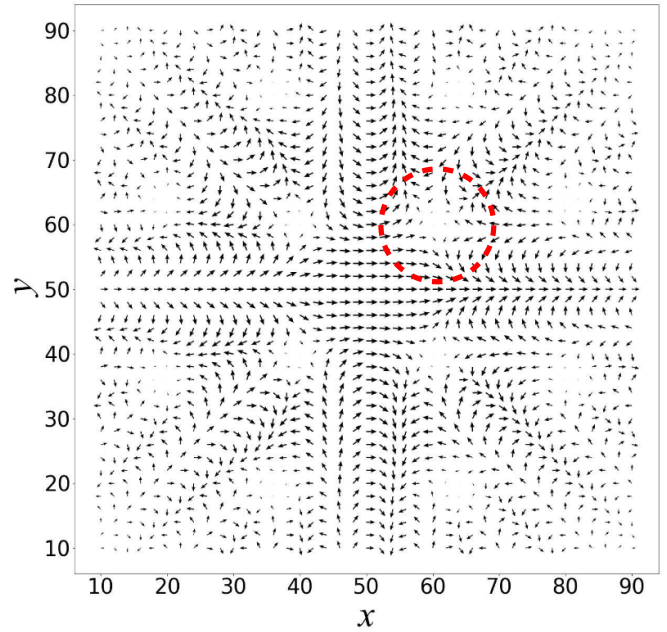

Figure 2. Numerical solution of polarization in response to magnetic field produced by a pairs of opposed Helmholz coils. The black arrows show the distribution of $\boldsymbol{P}$ that forms a anti-vortex crystal. The red dash-line circle marks one of the anti-vortices. The parameters are $\lambda = 3$, $\eta = 1$, $h = 0.12$ and $N = 100$.
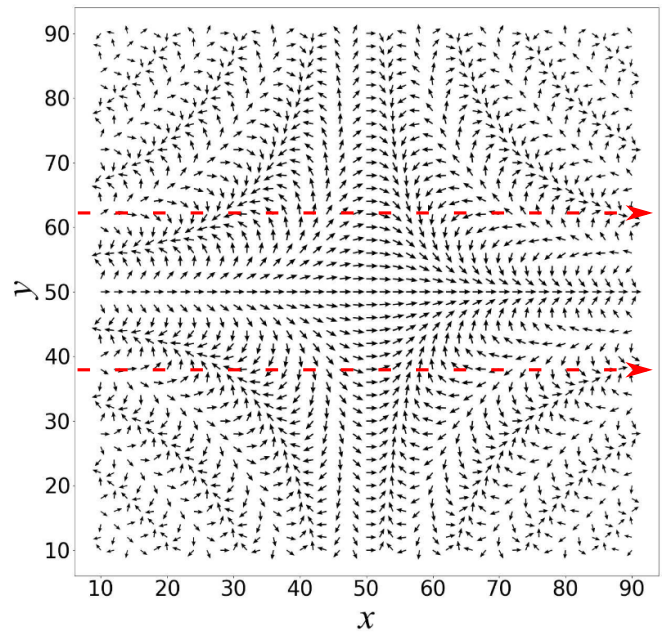

Figure 3. The polarization distribution with in-plane magnetic field solved numerically with parameters $\lambda = 4$, $\eta = 1$, $h = 0.12$ and $N = 100$. The red dash-line arrows show the track of the spiral orders, where the $\boldsymbol{P}$ rotates clockwise and anti-clockwise, respectively along top and bottom lines.

as $\vec{A}_x = \gamma(0,0,x)$, $\vec{A}_y = \gamma(0,0,y)$, $\vec{A}_z = \gamma(-x,-y,0)$, and $\vec{A}_0 = 0$. The numerical solution in this case gives us the distribution of $\boldsymbol{P}$ as shown in figure 4. There a bob of nearly parallel polarizations appear in a domain at the center of
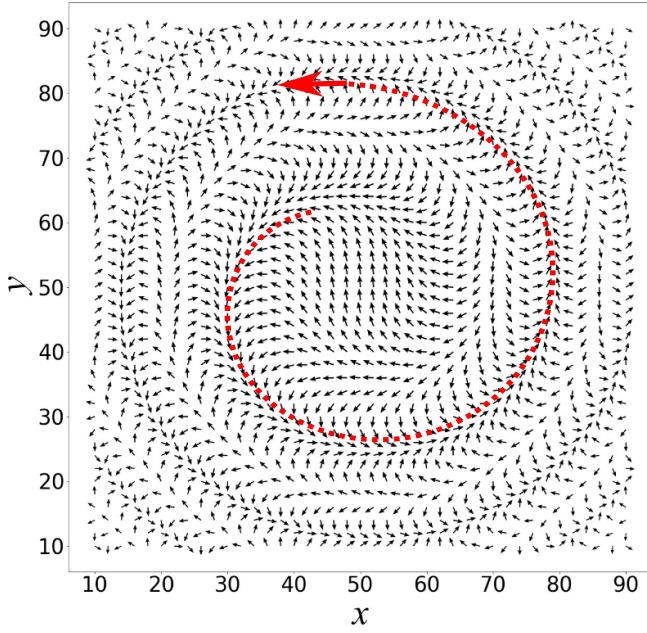
Figure 4. Numerical solution of the polarization distribution in the presence of magnetic field with non-vanishing curl. The red dash-line arrow shows a whirling track of spiral orders. The parameter choices are $\lambda = 4$, $\eta = 1$, $h = 0.12$ and $N = 100$.

the sample, and away from the domain, the polarization vectors change their directions gradually forming certain pattern. Such pattern contains a spatial spiral (marked by red dash-line arrow) tipping from the domain wall of the bob and whirling anti-clockwise.

4. More solutions for constant gauge potentials

A constant gauge potential is meaningless in abelian case, however, it becomes meaningful in nonablelian case. In the following, we exhibit two typical cases.

4.1. Spiral-type solutions

Let us consider $\vec{A}_x = (0, 0, b_2)$, $\vec{A}_z = (b_2, 0, 0)$ and $\vec{A}_y = \vec{A}_0 = 0$, i.e. $\mathcal{A}_x = b_2 \tau^3$, $\mathcal{A}_z = b_2 \tau^1$, and $\mathcal{A}_y = \mathcal{A}_0 = 0$. This implies a non-vanishing strength tensor, $F^y{}_{xz} = -F^y{}_{zx} = -b_2^2$. The free energy density (2) then becomes,

$$\mathcal{F} = \frac{1}{2} |(\nabla_x + b_2 \tau^3)\Psi|^2 + \frac{1}{2} |\nabla_y \Psi|^2 + \frac{b_2^2}{2} |\tau^1 \Psi|^2 + \frac{\lambda^2}{2} (|\Psi|^2 - \eta^2)^2 - \frac{1}{2} b_2^4. \quad (15)$$

As focusing on two-dimensional solutions merely, we treat the order parameter Ψ as independent of spatial variable z, i.e. $\nabla_z \Psi = 0$ and take $z = 0$ if it appears in the gauge potential. Now we have a solution

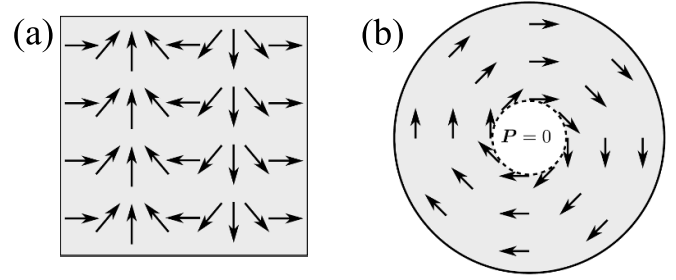$$\Psi = \frac{C}{\sqrt{2}} \begin{pmatrix} e^{-ib_2 x/2} \\ e^{ib_2 x/2} \end{pmatrix}$$

Figure 5. Schematic illustration of analytical solution for the polarization distribution where arrows represent the polarization direction. (a) The spiral-type solution for $\mathcal{A}_x = b_2 \tau^3$, $\mathcal{A}_z = b_2 \tau^1$. (b) Vortex-like solution for $\mathcal{A}_x = 2g\tau^1$, $\mathcal{A}_y = 2g\tau^2$, which is obtained for a round sample of radius R in which the small blank area refers to the vortex core with vanishing polarization.

with coefficient $C = \sqrt{\eta^2 - (b_2/\lambda)^2/4}$ that minimizes the above free energy (15). This solution gives rise to the following polarization of spiral-type orders along x-axis:

$$P_1 = C\cos(b_2 x),$$
$$P_2 = C\sin(b_2 x),$$

uniforming along y-axis. Figure 5(a) shows this solution in the region between $x = 0$ and $x = 2\pi/b_2$ schematically.

4.2. Vortex-like solutions

We consider further case $g_1 = g_2 = 2g$, i.e. $\mathcal{A}_x = 2g\tau^1$, $\mathcal{A}_y = 2g\tau^2$, and $\mathcal{A}_z = \mathcal{A}_0 = 0$, of which the non-vanishing field strength tensor is $F^z{}_{xy} = -F^z{}_{yx} = -4g^2$. The free energy density (2) is then given by

$$\mathcal{F} = \frac{1}{2} \sum_{i=1,2} |(\nabla_i + 2g\tau^i)\Psi|^2 + \frac{\lambda^2}{2}(|\Psi|^2 - \eta^2)^2 - 8g^4. \quad (16)$$

The sample is supposed to be a round disc of radius R in the x–y plane. Minimizing the above free energy under the homogeneous approximation (i.e. Ψ is regarded as constant), we get $|\boldsymbol{P}| = \eta^2 - g^2/\lambda^2$. Clearly, the module of the polarization depends on the strength g of the field, being nonzero only for $\eta^2 > g^2/\lambda^2$. To include the spatial variation of the polarization, we propose a 'trial wavefunction' with the order parameters being $\Psi = \left(a_1 e^{i\theta n_1 + i\phi}, a_2 e^{i\theta n_2}\right)^T$ where the superscript T denotes matrix transpose. Here n_1 and n_2 are integers; a_1 and a_2 are functions of the radial coordinate r. Substituting the aforementioned form of Ψ into equation (16) and then minimizing the free energy (16), we obtain a solution for the order parameter Ψ (see the detailed derivation in appendix). This solution gives rise to the distribution of polarization: $P_3 = 0$, and the in-plane components,

$$P_1 = (\eta^2 - g^2/\lambda^2)\cos(\theta - \pi/2),$$
$$P_2 = (\eta^2 - g^2/\lambda^2)\sin(\theta - \pi/2),$$

for $r > \xi$; but $P_1 = P_2 = 0$ for $r < \xi$. This is a polar vortex with a vortex core of radius ξ and is exhibited schematically in

figure 5(b). Here ξ is obtained by minimizing $\Delta\mathcal{F} = \pi(\eta^2 - g^2/\lambda^2)\left[(\lambda^2\eta^2 - g^2)\xi^2/2 - g^2(R-\xi)^2/\ln(R/\xi)\right]$, where $\Delta\mathcal{F}$ is the free energy difference between the vortex solution and the homogeneous solution. The result $\Delta\mathcal{F} < 0$ means that the system always favors a vortex. Recently, the coexistence of polar vortices with certain complex-phase and their response under applied electric fields in superlattices of $(\text{PbTiO3})_n/(\text{SrTiO3})_n$ have indeed been observed [7].

5. Revisit thermodynamics

To revisit thermodynamics, we take uniform order parameter (i.e. $\nabla_i\Psi = 0$) and electric field $\boldsymbol{E}$ in the free energy (2). Clearly, the dielectric material corresponds to the special case $\eta = 0$, of which the free energy reads $\mathcal{F} = \frac{1}{2}\lambda^2|\Psi|^4 - \boldsymbol{E}\cdot\Psi^\dagger\boldsymbol{\sigma}\Psi$ giving rise to $\boldsymbol{P} = 2/\lambda^2\boldsymbol{E}$. This means $8\pi/\lambda^2 = \varepsilon - 1$ with ε being the dielectric constant of isotropic medium. One can also take account of the spatial components in equation (9), saying $b_2 \neq 0$ (for Gauss unit $b_2 = 1/\sqrt{4\pi}$). For simplicity, choosing the direction of electric field as x-axis that implies $\vec{A}_0 = (E, 0, 0)$, one obtain from the definition (3) non-vanishing strength tensors $F^y_{0x} = -F^y_{x0} = E/\sqrt{4\pi}$ and $F^y_{xz} = -F^y_{zx} = -(4\pi)^{-1}$. Then the free energy (2) becomes

$$\mathcal{F} = \mathcal{F}_0 - E\Psi^\dagger\sigma^x\Psi - \frac{1}{8\pi}E^2 \qquad (17)$$

where the zero field terms

$$\mathcal{F}_0 = U(|\Psi|) + \frac{1}{8\pi}\left(|\tau^3\Psi|^2 + |\tau^1\Psi|^2 + \frac{1}{\pi}\right)$$

are the uniform case of equation (15). Then the electric displacement $D = E + 4\pi P$ can be derived via the well known thermodynamics relation

$$D = -4\pi\left(\frac{\partial\mathcal{F}}{\partial E}\right)_T.$$

Since we focused on very low temperature $T \ll T_0$ in studying those solutions in the above, we had taken coefficient of Landau's temperature expansion $a_0(T - T_0)$ simply as $-\eta^2\lambda^2$ and had not taken account of higher order terms of electric polarization. To describe the so-called proper ferroelectric more precisely at finite temperature, particularly, closing to the transition temperature, higher order terms in $U(|\Psi|)$ become necessary.

Furthermore, if extending present theoretical frame to $SU(2) \times SU(2)$ by an additional order parameter

$$\Psi' = \left(\begin{array}{c} \eta_1 \\ \eta_2 \end{array}\right)$$

where η_1 and η_2 are complex functions in general, we will naturally have the following free energy for improper ferroelectric

$$\begin{aligned} \mathcal{F}' =\,& a(T - T_c)\Psi'^\dagger\Psi' + B(\Psi'^\dagger\Psi')^2 + C_{ij}P'_iP_j \\ & + \frac{\lambda^2}{2}\boldsymbol{P}^2 - \boldsymbol{E}\cdot\boldsymbol{P} - \frac{1}{8\pi}\boldsymbol{E}^2 \end{aligned} \qquad (18)$$

where $\boldsymbol{P}$ was defined by equation (4) and $\boldsymbol{P}' = \Psi'^\dagger\boldsymbol{\sigma}\Psi'$ namely, $P'_x = \eta_1^*\eta_2 + \eta_2^*\eta_1$, $P'_y = i(\eta_2^*\eta_1 - \eta_1^*\eta_2)$, $P'_z = \eta_1^*\eta_1 - \eta_2^*\eta_2$. The expression in reference [32] corresponds to $C_{zx} = -C_{xy} = C_1$, $C_{zy} = C_{xx} = C_2$ with restriction of real order parameter that implies $P'_y = 0$.

6. Discussion and outlook

Ferroelectricity [2] can be defined as the electric analog of ferromagnetism [32], of which the fundamental criterion is the existence of hysteresis, i.e. the static electric displacement depends not only on the applied electric field but also on the past history of the material. The traditional theory is based on the free energy of equation (1) that is a function of variable P, $\mathcal{F}_{\text{LD}} = \mathcal{F}(P)$ and its variational derivative $\delta\mathcal{F}_{\text{LD}}/\delta P = 0$ gives rise to $E = -2\alpha P + 4\beta P^3$. Introducing a two-component order parameter Ψ, we proposed a macroscopic phenomenological theory for ferroelectricity in the spirit of GL formalism for superconductors. Since the free energy in our theory is a functional of the complex order parameter, i.e. $\mathcal{F} = \mathcal{F}(\Psi, \Psi^\dagger)$, and the electric polarization is defined as quadratic form of the order parameter, there is always remanent polarization as long as $\eta \neq 0$. Additionally, such an order parameter defines a charge complex plane and the independence of the choice of the bases naturally implies the existence of a SU(2) gauge potential. The nonabelian feature of SU(2) then automatically involves the interplays between several degree of freedoms. Considering the presence of either temporal or spatial component of the gauge potential, we obtained several solutions in the theory, of which some have been created in experiments [7, 11]. It will be also interesting to apply our theory to understand the recently observed polar skyrmions [8] or to search more possible exotic polarization topologies [9].

The research enthusiasm on multiferroics, the phenomena that magnetism and ferroelectricity coexist in certain solids [38–41], is driven by the prospect of controlling charges by applied magnetic fields [42, 43] and spins by applied voltages [44]. To directly extend the Landau-Devonshire theory to describe multiferroics, one has to add, by hand, the coupling between magnetization and polarization vectors [23, 41]. Note that a spin SU(2) together with the charge U(1) was considered [45] in a theoretical understanding of the fractional quantum Hall effects, and later considered [46] in exploring spin superfluidity. To include magnetic orders [47], this might cue us to extend the present formalism to high-rank groups, saying $SU_{\text{polar}}(2) \times SU_{\text{spin}}(2)$. Whereas, there is another passage for the same purpose. Actually, the nonabelian gauge potential A_μ^a in present macroscopic theory implies more degree of freedoms. The SU(2) gauge potential contains totally twelve parameters while the U(1) gauge contains four only. In a novel decomposition [48] of the SU(2) gauge potential that A_μ^3 was considered as a U(1) gauge field and $A_\mu^\pm = A_\mu^1 \pm iA_\mu^2$ as vector field, the author formulated a nonlinear sigma-model with unit vector $\boldsymbol{m}(\boldsymbol{r})$ which is an example of baby Skyrme model [49]. This may be a possible clue to formulate a macroscopic theory for spin originated [47] polarizations in the future.

Data availability statement

All data that support the findings of this study are included within the article.

Acknowledgment

Author contributions

Y Q L proposed the formulism and conducted the study; H Z, H Z, L B F participated frequent discussion at earlier stage; P W contributed calculation obtaining the vortex-like solution and numerical simulations.

Conflict of interest

The authors declare no competing interests.

Appendix A. Formulae for numerical solutions

For the purpose of numerical calculations, we introduce virtual time t acting as a relaxation parameter. For the total free energy

$$\mathfrak{F} = \int \mathcal{F} \mathrm{d}^3 r \qquad \text{(A1)}$$

which is the functional integrand of the order parameters Ψ, $\Psi^\dagger$ and gauge potentials A_μ^a. The variational principle, $\partial \Psi / \partial t = -\delta \mathfrak{F}/\delta \Psi^\dagger$, together with $\partial A_\mu^a / \partial t = -\delta \mathfrak{F}/\delta A_\mu^a$ give rise to the following equations of motion,

$$\left(\frac{\partial}{\partial t} + i A_0^a \tau^a \right) \Psi = \lambda^2 (\eta^2 - |\Psi|^2) \Psi + \frac{1}{2} \left(\partial_i + A_i^a \tau^a \right)^2 \Psi,$$

$$\frac{\partial}{\partial t} A_\mu^a = \left(\partial_\nu F^a{}_{\mu\nu} - \epsilon^{abc} A_\nu^b F^c{}_{\mu\nu} \right) + J_\mu^a \qquad \text{(A2)}$$

where the polarization four-currents are given by

$$J_0^a = \Psi^\dagger \tau^a \Psi,$$

$$J_i^a = \frac{1}{2} \left[(\partial_i \Psi)^\dagger \tau^a \Psi - \Psi^\dagger \tau^a \partial_i \Psi \right] + \frac{1}{4} |\Psi|^2 A_i^a. \qquad \text{(A3)}$$

In deriving the above results, we used the fact that $(\tau^a)^\dagger = -\tau^a$. The time evolution equation (A2) are very useful for searching a steady solution numerically from a proper trial 'initial' order parameter. The second term in above equation can be regarded as the analogy of London equation in the GL phenomenology theory for superconductors.

In our numerical calculation, we consider a two-dimensional sample located in the x–y plane and hence take $\partial_z \Psi = 0$ and $z = 0$ when evaluating the free energy. The gauge potential $A_\mu^a(x, y)$ which is determined by the external elec-

tric and magnetic fields, is fixed in this paper, i.e. we set $\partial A_\mu^a / \partial t = 0$ in the virtual-time evolution. Discretizing the x–y plane into a square lattice of edge Nh for lattice constant h and a large integer N (e.g. $N = 100$), we numerically solve the first one of equation (A2) till a large enough t so that $|\partial \Psi / \partial t|^2$ is below a threshold magnitude ε which is set in advance. We choose a small ε, hence, Ψ at the end of evolution is a good approximation of its steady solution, i.e. the minimum point of $\int \mathcal{F} \mathrm{d}x \mathrm{d}y$. Different initial Ψ's have been also tested to guarantee that what we obtain is the global minimum.

Appendix B. Derivations for analytical solutions

In the following, we give our derivations on several analytical solutions in detail. Two situations, (a) $\mathcal{A}_0 \neq 0$, $\mathcal{A}_i = 0$ and (b) $\mathcal{A}_i \neq 0$ while $\mathcal{A}_0 = 0$ are investigated successively.

B.1. The case $\mathcal{A}_0 \neq 0$ while $\mathcal{A}_i = 0$

In this case, the free energy is expressed as

$$\mathcal{F} = \int \mathrm{d}^3 r \left[\sum_{i=1,2} \frac{1}{2} \mid \nabla_i \Psi \mid^2 + U(|\Psi|^2) - E^a \Psi^\dagger \sigma^a \Psi \right]. \quad \text{(B1)}$$

B.1.1. Electric field produced by a charged line.
We first consider an external electric field given in equation (12) that can be produced by a charged line perpendicular to the x–y plane. As the external field is of axial symmetric, we employ the polar coordinates (r, θ) and consider the sample to be a round disc in the two-dimensional plane with the center being at the origin. In general, it will be a hard task to minimize the free energy (B1) for a two-component complex order parameter Ψ. As a crucial step, we consider it be of axial symmetric by assuming the following form

$$\Psi = \begin{pmatrix} a_1(r) \, \mathrm{e}^{i n_1 \theta + i \phi} \\ a_2(r) \, \mathrm{e}^{i n_2 \theta} \end{pmatrix} \qquad \text{(B2)}$$

where r and θ denote the radial coordinate and the azimuthal angle, respectively, and $a_1(r)$ and $a_2(r)$ are real functions to be determined. Here n_1 and n_2 must be integers so that the Ψ is single-valued at every point, and ϕ ($0 \leqslant \phi < 2\pi$) is a constant that refers the phase difference between the two components of Ψ. The ansatz (B2) greatly simplifies our problem of minimizing the free energy $\mathcal{F}$, meanwhile keeping the possibility of expressing abundant topological structures in the polarization distribution.

In terms of the expression (B2), the polarization is given by

$$P_1 = 2 a_1 a_2 \cos \left[(n_2 - n_1) \theta - \phi \right],$$

$$P_2 = 2 a_1 a_2 \sin \left[(n_2 - n_1) \theta - \phi \right],$$

$$P_3 = a_1^2 - a_2^2, \qquad \text{(B3)}$$

and the free energy turns to be

$$
\begin{aligned}
\mathcal{F}(n_1, n_2) = \frac{1}{2} \int_0^R \mathrm{d}r\, r \int_0^{2\pi} \mathrm{d}\theta \Big[&\dot{a}_1^2 + \dot{a}_2^2 \\
&+ \frac{1}{r^2} \left(n_1^2 a_1^2 + n_2^2 a_2^2 \right) + \lambda^2 \left(a_1^2 + a_2^2 - \eta^2 \right)^2 \\
&- 4\gamma \frac{a_1 a_2}{r} \cos\left[\theta \left(n_2 - n_1 - 1 \right) - \phi \right] \Big],
\end{aligned} \tag{B4}
$$

where the overhead dot denotes derivative with respect to r for simplicity in expression, i.e. $\dot{a}_1 = \mathrm{d}a_1/\mathrm{d}r$ and $\dot{a}_2 = \mathrm{d}a_2/\mathrm{d}r$. Clearly, we need to discuss the cases of $n_2 - n_1 = 1$ and $n_2 - n_1 \neq 1$ separately. For $n_2 - n_1 \neq 1$, the integrand of the last term in equation (B4) taken over θ vanishes. It is straightforward that $\mathcal{F}(n_1, n_2)$ takes its minimum when $n_1 = n_2 = 0$. Thus $\mathcal{F}(0,0)$ is nonnegative and takes its minimum value $\mathcal{F}(0,0) = 0$ if and only if $a_1^2 + a_2^2 = \eta^2$ with a_1 and a_2 being constants (i.e. $\dot{a}_1 = \dot{a}_2 = 0$). When $n_2 - n_1 = 1$, the free energy can be negative due to the contribution from the last term in equation (B4). In this case, the free energy reads

$$
\begin{aligned}
\mathcal{F}(n_1) = \pi \int_0^R \mathrm{d}r\, r \Big[&\dot{a}_1^2 + \dot{a}_2^2 + \frac{1}{r^2} \left(n_1^2 a_1^2 + (n_1 + 1)^2 a_2^2 \right) \\
&+ \lambda^2 \left(a_1^2 + a_2^2 - \eta^2 \right)^2 - 4\gamma \cos\phi \frac{a_1 a_2}{r} \Big].
\end{aligned} \tag{B5}
$$

Thus either $n_1 = 0$ or $n_1 = -1$ minimizes the free energy (B5). Consequently, one component of Ψ has a constant phase, while the other's phase shifts by 2π once a circle. The contribution from the third term of equation (B5) can be neglected at large r since it decays much faster than the γ-term due to the factor $1/r^2$. To minimize $\mathcal{F}$, we obviously need to take $\dot{a}_1, \dot{a}_2 \to 0$ and $a_1^2 + a_2^2 \to \eta^2$ in the limit $r \to \infty$. If the radius R of the sample is large enough, the first three terms in equation (B5) can then be neglected and the fourth term should equal to zero. It is then easy to see that $a_1 = a_2 = \eta/\sqrt{2}$ and $\phi = 0$ (if $\gamma > 0$) or $\phi = \pi$ (if $\gamma < 0$) minimize $\mathcal{F}$. Thus the free energy $\mathcal{F}(n_1, n_1 + 1) \approx -2\pi R |\gamma| \eta^2$ is negative. Recalling that the minimum free energy for the case $n_2 - n_1 \neq 1$ is zero, we conclude that the solution with $n_2 = n_1 + 1$ is more favorite in free energy. This solution gives rise to the following polarization

$$
\begin{aligned}
P_1 &= \pm \eta^2 \cos\theta, \\
P_2 &= \pm \eta^2 \sin\theta, \\
P_3 &= 0,
\end{aligned} \tag{B6}
$$

where the sign ' $+$ ' and ' $-$ ' hold for $\gamma > 0$ and $\gamma < 0$ respectively. It is worthwhile to mention that the above expression of polarization is correct only for the place far away from the origin. We do not analyze how the polarization changes when one goes close to the origin.

B.1.2. Curling electric field. For a curling electric field given in equation (13) that can be produced by applying alternative electric current in a thin solenoid placed in perpendicular to

the x–y plane, we take the same Ψ ansatz of (B2) and obtain the free energy as follows

$$
\begin{aligned}
\mathcal{F} = \frac{1}{2} \int_0^R \mathrm{d}r\, r \int_0^{2\pi} \mathrm{d}\theta \Big[&\dot{a}_1^2 + \dot{a}_2^2 + \frac{1}{r^2} \left(n_1^2 a_1^2 + n_2^2 a_2^2 \right) \\
&+ \lambda^2 \left(a_1^2 + a_2^2 - \eta^2 \right)^2 - 4\gamma \frac{a_1 a_2}{r} \\
&\times \sin\left[\theta \left(n_2 - n_1 - 1 \right) - \phi \right] \Big].
\end{aligned} \tag{B7}
$$

The minimum point of the above free energy solves $n_2 = n_1 + 1$, $a_1 = a_2 = \eta/\sqrt{2}$ and either $\phi = -\pi/2$ (if $\gamma > 0$) or $\phi = \pi/2$ (if $\gamma < 0$). This solution gives rise to the following polarization

$$
\begin{aligned}
P_1 &= \eta^2 \cos\left(\theta \pm \pi/2 \right), \\
P_2 &= \eta^2 \sin\left(\theta \pm \pi/2 \right), \\
P_3 &= 0,
\end{aligned} \tag{B8}
$$

in which one takes ' $+$ ' or ' $-$ ' depending on $\gamma > 0$ or $\gamma < 0$.

B.2. The case $\mathcal{A}_i \neq 0$ while $\mathcal{A}_0 = 0$

For the second case $\mathcal{A}_i \neq 0$ while $\mathcal{A}_0 = 0$, we consider the gauge field to be $\mathcal{A}_1 = 2g\tau^1$, $\mathcal{A}_2 = 2g\tau^2$ and $\mathcal{A}_3 = 0$ where g is a constant. Let us focus on the case of $g^2 < \eta^2 \lambda^2$, in which there exists a nonzero Ψ. The gauge field is now a constant and the sample is assumed to be round-shaped, thus the solution Ψ possesses axial symmetry and is still considered to take the ansatz form of equation (B2). The covariant derivative in the polar coordinates is now evaluated as

$$
\begin{aligned}
&|D_1 \Psi|^2 + |D_2 \Psi|^2 \\
&= \dot{a}_1^2 + \dot{a}_2^2 + \frac{1}{r^2} \left(n_1^2 a_1^2 + n_2^2 a_2^2 \right) + 2g^2 \left(a_1^2 + a_2^2 \right) \\
&\quad + 2g \sin\left[\left(n_1 - n_2 + 1 \right) \theta + \phi \right] \\
&\quad \times \left(a_2 \dot{a}_1 - a_1 \dot{a}_2 - \frac{a_1 a_2}{r} \left(n_1 + n_2 \right) \right).
\end{aligned} \tag{B9}
$$

The integral over the polar coordinates is expressed as $\int_0^{2\pi} \mathrm{d}\theta \int_0^R \mathrm{d}r\, r$ where R is the radius of the sample. The free energy needs to be discussed for the cases of $n_2 - n_1 = 1$ and $n_2 - n_1 \neq 1$ separately.

When $n_2 - n_1 \neq 1$, the integrand of the last term of equation (B9) with respect to θ vanishes and the free energy becomes

$$
\begin{aligned}
\mathcal{F}(n_1, n_2) = \pi \int_0^R \mathrm{d}r\, r \Big[&\dot{a}_1^2 + \dot{a}_2^2 + \frac{1}{r^2} \left(n_1^2 a_1^2 + n_2^2 a_2^2 \right) \\
&+ \left(2g^2 - 2\lambda^2 \eta^2 \right) \left(a_1^2 + a_2^2 \right) + \lambda^2 \left(a_1^2 + a_2^2 \right)^2 \Big].
\end{aligned} \tag{B10}
$$

Since $\left(n_1^2 a_1^2 + n_2^2 a_2^2 \right)/r^2$ is always nonnegative, $\mathcal{F}(n_1, n_2)$ must take its minimum at $n_1 = n_2 = 0$. It is straightforward to see that the minimization of equation (B10) leads to $\dot{a}_1 = \dot{a}_2 = 0$ (i.e. a_1 and a_2 are constants) and $|\Psi|^2 = a_1^2 + a_2^2 = \eta^2 - g^2/\lambda^2$

since $g^2 < \eta^2\lambda^2$. Thus the minimum value of the free energy is

$$\mathcal{F}(0,0) = \pi R^2 \frac{-\lambda^2}{2}\left(\eta^2 - g^2/\lambda^2\right)^2 \tag{B11}$$

where πR^2 is the area of the sample. In fact, $n_1 = n_2 = 0$ corresponds to a uniform polarization without vortex.

When $n_2 - n_1 = 1$, the free energy becomes

$$
\begin{aligned}
&\mathcal{F}(n_1, n_1+1) \\
&= \pi \int_0^R \mathrm{d}r\, r\Bigg[\dot{a}_1^2 + \dot{a}_2^2 + \left(2g^2 - 2\lambda^2\eta^2\right)\left(a_1^2 + a_2^2\right) \\
&\quad + \lambda^2\left(a_1^2 + a_2^2\right)^2 + \frac{1}{r^2}\left(n_1^2 a_1^2 + (n_1+1)^2 a_2^2\right) \\
&\quad + 2g\sin\phi\left(a_2\dot{a}_1 - a_1\dot{a}_2 - \frac{a_1 a_2}{r}(2n_1+1)\right)\Bigg].
\end{aligned}
\tag{B12}
$$

As will be shown, the last term is negative, leading to $\mathcal{F}(n_1, n_1+1) < \mathcal{F}(0,0)$. Therefore, $n_2 = n_1 + 1$ is indeed the global minimum point.

It is obvious that $a_1, a_2 \to 0$ in the limit $r \to 0$, otherwise, the integral in equation (B12) would be divergent. The variational principle $\delta\mathcal{F} = 0$ gives rise to second order differential equations:

$$
\begin{aligned}
\frac{\mathrm{d}^2 a_1}{\mathrm{d}r^2} &= \left[\frac{n_1^2}{r^2} + 2g^2 - 2\lambda^2\eta^2 + 2\lambda^2\left(a_1^2 + a_2^2\right)\right]a_1 \\
&\quad - \frac{1}{r}\frac{\mathrm{d}a_1}{\mathrm{d}r} + g\sin\phi\left[-2\frac{\mathrm{d}a_2}{\mathrm{d}r} - \frac{2n_1+2}{r}a_2\right], \\
\frac{\mathrm{d}^2 a_2}{\mathrm{d}r^2} &= \left[\frac{(n_1+1)^2}{r^2} + 2g^2 - 2\lambda^2\eta^2 + 2\lambda^2\left(a_1^2 + a_2^2\right)\right]a_2 \\
&\quad - \frac{1}{r}\frac{\mathrm{d}a_2}{\mathrm{d}r} + g\sin\phi\left[2\frac{\mathrm{d}a_1}{\mathrm{d}r} - \frac{2n_1}{r}a_1\right].
\end{aligned}
\tag{B13}
$$

On the one hand, in the limit $r \to 0$, we assume $a_1 \propto r^{\alpha_1}$ and $a_2 \propto r^{\alpha_2}$ and substitute them into equation (B13). Here only the leading terms on both sides of equation (B13) are kept (e.g. in the presence of r^{α_1-2} term, r^{α_1} and r^{α_1-1} can be neglected because they tend to zero much faster). By comparing the leading terms in the left- and right-hand sides of the equation, we find $\alpha_1 = |n_1|$ and $\alpha_2 = |n_1 + 1|$. On the other hand, in the region far away from the origin (in the limit $r \to \infty$), the terms with the factor $1/r^2$ or $1/r$ in equations (B12) and (B13) can be neglected. It is then reasonable to assume $\dot{a}_1, \dot{a}_2 \to 0$ that means the order parameter distributes uniformly in the bulk except slight variations merely at the vicinity of the origin. To minimize the free energy far away from the origin, we need to let $a_1^2 + a_2^2 = \eta^2 - g^2/\lambda^2$ with a_1 and a_2 being constants. Without loss of generality, we set $a_1(r \to \infty) = \cos\chi\sqrt{\eta^2 - g^2/\lambda^2}$ and $a_2(r \to \infty) = \sin\chi\sqrt{\eta^2 - g^2/\lambda^2}$ with χ being a tunable parameter. All together, a_1 (or a_2) should

approach to r^{α_1} (or r^{α_2}) in the limit $r \to 0$ and approach to a constant in the limit $r \to \infty$. We thus assume

$$
\begin{aligned}
a_1 &= \left(1 - \mathrm{e}^{-\left(\frac{r}{\xi}\right)^{\alpha_1}}\right)\sqrt{\eta^2 - g^2/\lambda^2}\cos\chi, \\
a_2 &= \left(1 - \mathrm{e}^{-\left(\frac{r}{\xi}\right)^{\alpha_2}}\right)\sqrt{\eta^2 - g^2/\lambda^2}\sin\chi,
\end{aligned}
\tag{B14}
$$

where ξ is a tunable parameter referring to the radius of the vortex core.

Substituting equation (B14) into equation (B12), we are able to calculate the free energy and conveniently consider $\Delta\mathcal{F} = \mathcal{F}(n_1, n_1+1) - \mathcal{F}(0,0)$ that is the free energy difference between the vortex solution and the uniform solution. Clearly, the system favors a vortex solution if $\Delta\mathcal{F} < 0$ while it favors a uniform polarization if $\Delta\mathcal{F} > 0$. According to equation (B12), $\Delta\mathcal{F}$ is an integral with respect to r and the integrand contains several terms. Some of them decay exponentially ($\sim \mathrm{e}^{-\left(\frac{r}{\xi}\right)^{\alpha_{1,2}}}$), thereafter, the integral $\int_0^R \mathrm{d}r$ can be replaced by $\int_0^\infty \mathrm{d}r$ as if R is larger than several times of ξ. We will show later that such a condition $\xi/R \ll 1$ is indeed satisfied. The other terms either decay much slowly ($\sim 1/r$) or do not decay at all. The integrand of these terms are proportional to $\ln R$ or R, respectively. Note that the last term in the integrand gives rise to $-2g\sin\phi\, a_1 a_2(2n_1+1)$, therefore, n_1 here should be a large integer so as to minimize $\Delta\mathcal{F}$. It will be shown that the value of n_1 indeed satisfies $n_1 \gg 1$ when the sample's radius R is large enough. Under these two conditions (i.e. $n_1 \gg 1$ and $R \gg \xi$), we obtain

$$
\begin{aligned}
\Delta\mathcal{F} &= \pi\left(\eta^2 - g^2/\lambda^2\right)\Bigg[\frac{n_1}{4} + \frac{\sin^2\chi}{4} + \left(\lambda^2\eta^2 - g^2\right)\frac{\xi^2}{2} \\
&\quad + n_1^2\cos^2\chi\left(\ln\frac{R}{\xi} + \frac{C - \ln 2}{n_1}\right) \\
&\quad + (n_1+1)^2\sin^2\chi\left(\ln\frac{R}{\xi} + \frac{C - \ln 2}{n_1+1}\right) \\
&\quad - 2g\sin\phi\sin\chi\cos\chi\,(2n_1+1)\,(R - \xi)\Bigg]
\end{aligned}
\tag{B15}
$$

where $C = 0.577\ldots$ is the Euler constant. In the calculation, we have used $\alpha_1 = n_1$, $\alpha_2 = n_1 + 1$ ($n_1 > 0$), $\mathrm{e}^{-\left(\frac{r}{\xi}\right)^{\alpha_1} - \left(\frac{r}{\xi}\right)^{\alpha_2}} \approx \mathrm{e}^{-2\left(\frac{r}{\xi}\right)^{\alpha_1}}$ and $\int_0^\infty \mathrm{d}r\, r\, \mathrm{e}^{-\left(\frac{r}{\xi}\right)^{\alpha_1}} = \frac{\xi^2}{\alpha_1}\Gamma\left(\frac{2}{\alpha_1}\right) = \frac{\xi^2}{2}\Gamma\left(\frac{2}{\alpha_1} + 1\right) \approx \frac{\xi^2}{2}$ for $\alpha_1 \gg 1$, and $\lim_{\epsilon \to 0^+}\mathrm{Ei}(-\epsilon) - \ln\epsilon = C$. Here $\Gamma(x) = \int_0^\infty \mathrm{d}t\, \mathrm{e}^{-t}t^{x-1}$ is the gamma function and $\mathrm{Ei}(x) = -\int_{-x}^\infty \mathrm{d}t\, \mathrm{e}^{-t}t^{-1}$ is the exponential integral function.

We are in the position to minimize $\Delta\mathcal{F}$ in equation (B15) with respect to the variables ϕ, χ, ξ and n_1. In equation (B15), $n_1/4$, and $\sin^2\chi/4$ are much smaller than the other terms due to $n_1 \gg 1$. Similarly, $(C - \ln 2)/n_1$ is much smaller than $\ln R/\xi$. Thus these terms can be neglected. Without loss of generality, we choose $b > 0$ and $\sin\chi\cos\chi > 0$, and then obtain $\sin\phi = 1$, namely,
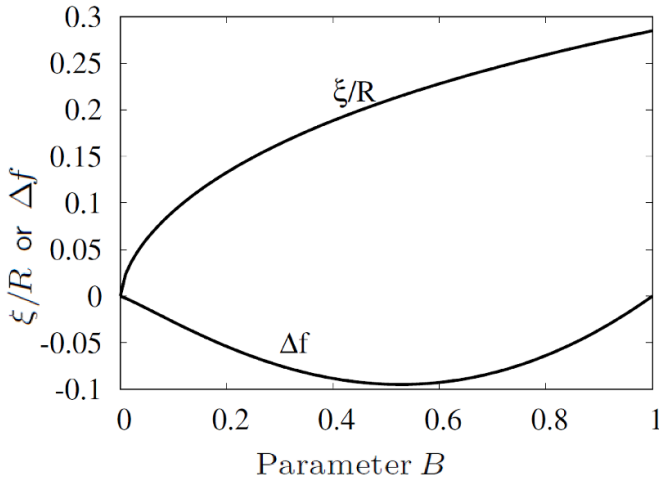
Figure 6. Parameter dependance of vortex core and free energy density. The ratio of the vortex-core radius to the sample radius (ξ/R) as a function of the renormalized field $B = g^2/(\lambda^2\eta^2)$. The corresponding free energy density $\Delta f = \Delta F/(\pi R^2)$ in unit of $\lambda^2\eta^4$ is also plotted.

$$\phi = \pi/2. \tag{B16}$$

The value of χ is determined by $\partial\Delta\mathcal{F}/\partial\chi = 0$ and hence

$$\sin 2\chi = \frac{2g(R-\xi)}{\sqrt{\left(\ln\frac{R}{\xi}\right)^2 + 4g^2(R-\xi)^2}}. \tag{B17}$$

Now $\Delta\mathcal{F}$ is a quadratic form of n_1 and it takes the minimum at

$$2n_1 + 1 = \sqrt{1 + \frac{4g^2(R-\xi)^2}{\left(\ln\frac{R}{\xi}\right)^2}}. \tag{B18}$$

The condition $n_1 \gg 1$ suggests $2g(R-\xi)/\ln(\frac{R}{\xi}) \gg 1$. Under such a condition, we have $\chi \approx \pi/4$ and

$$\Delta\mathcal{F} \approx \pi\left(\eta^2 - g^2/\lambda^2\right)\left[\left(\lambda^2\eta^2 - g^2\right)\frac{\xi^2}{2} - \frac{g^2(R-\xi)^2}{\ln\frac{R}{\xi}}\right]. \tag{B19}$$

Minimizing the above expression (B19), we obtain ξ and the corresponding free energy difference. We plot in figure 6 the ratio ξ/R and the free energy density $\Delta f = \Delta F/(\pi R^2)$ as a function of the renormalized field $B = g^2/(\lambda^2\eta^2)$. Note that $g^2 < \eta^2\lambda^2$ and hence $B \in (0,1)$ for nonzero polarization. For arbitrary g, the sample's radius is at least three times of the vortex's radius, thereafter, our assumption $\xi/R \ll 1$ fulfills. As $\Delta\mathcal{F}$ is always negative, it manifests the existence of vortex solution. Choosing $\xi/R = 0.3$, we obtain $2g(R-\xi)/\ln(\frac{R}{\xi}) = 1.16gR$. Therefore, the condition $n_1 \gg 1$ fulfills if $gR \gg 1$. Actually, $n_1 \geqslant 10$ is enough for our approximation in the calculation of free energy to be a good one, which corresponds to $R \geqslant 18/g$. But for a weaker field, ξ/R is smaller, and gR has to be chosen sufficiently large.

Under the condition $n_1 \gg 1$, we have $\chi \approx \pi/4$ and $\sin\chi = \cos\chi = 1/\sqrt{2}$ and find that $P_3 \approx 0$ and the magnitude of P_1 and P_2 are quite different between in the regions $r > \xi$ and $r < \xi$, that is

$$\begin{aligned} P_1 &\approx \left(\eta^2 - g^2/\lambda^2\right)\cos(\theta - \tfrac{\pi}{2}), \\ P_2 &\approx \left(\eta^2 - g^2/\lambda^2\right)\sin(\theta - \tfrac{\pi}{2}), \end{aligned} \tag{B20}$$

for $r > \xi$; while for $r < \xi$

$$P_1 = P_2 = 0. \tag{B21}$$

Consequently, the polarization $\boldsymbol{P}$ vanishes inside the core of the vortex (when $r < \xi$) and it rotates clockwise in the x–y plane with a fixed length outside of the core. Similarly, for the other case, $g < 0$, the $\boldsymbol{P}$ rotates anticlockwise.

ORCID iDs

You-Quan Li ⬤ https://orcid.org/0000-0002-5243-2118
Hong Zhang ⬤ https://orcid.org/0000-0002-3273-5779

References

[1] Curie P 1894 *J. Phys.* **3** 393
[2] Devonshire A F 1954 Theory of ferroelectrics *Adv. Phys.* **3** 85–130
[3] Schmid H 1994 *Ferroelectrics* **162** 317
[4] Bussmann-Holder A 2020 Ferroelectrics past, present and future *Ferroelectrics* **569** 1
[5] Resta R 1992 Theory of the electric polarization in crystals *Ferroelectrics* **136** 51
[6] Resta R and Vanderbilt D 2007 *Physics of Ferroelectrics: A Modern Perspective* ed K Rabe, C H Ahn and J-M Triscone (Berlin: Springer) p 31
[7] Yadav A K *et al* 2016 Observation of polar vortices in oxide superlattices *Nature* **530** 198
[8] Das S *et al* 2019 Observation of room-temperature polar skyrmions *Nature* **568** 368
[9] Wang Y J *et al* 2020 Polar meron lattice in strained oxide ferroelectrics *Nat. Mater.* **19** 881
[10] Hong Z, Das S, Nelson C, Yadav A, Wu Y, Junquera J, Chen L Q, Martin L W and Ramesh R 2021 Vortex domain walls in ferroelectrics *Nano Lett.* **21** 3533
[11] Abid A Y *et al* 2021 Creating polar antivortex in PbTiO$_3$/SrTiO$_3$ superlattice *Nat. Commun.* **12** 2054
[12] Luo S and You L 2021 Skyrmion devices for memory and logic applications *APL Mater.* **9** 050901
[13] Hur N, Park S, Sharma P A, Ahn J S, Guha S and Cheong N-W 2004 Electric polarization reversal and memory in a multiferroic material induced by magnetic fields *Nature* **429** 392
[14] Ramesh R and Spaldin N A 2007 Multiferroics: progress and prospects in thin films *Nat. Mater.* **6** 21
[15] Harris A B 2007 Landau analysis of the symmetry of the magnetic structure and magnetoelectric interaction in multiferroics *Phys. Rev.* B **76** 054447
[16] Nahas Y, Prokhorenko S, Louis L, Gui Z, Kornev I and Bellaiche L 2015 Discovery of stable skyrmioinic state in ferroelectric nanocomposites *Nat. Commun.* **6** 8542
[17] Ruff E, Widmann S, Lunkenheimer P, Tsurkan V, Bordács S, Kézsmárki I and Loidl A 2015 Multiferroicity and skyrmions carrying electric polarization in GaV$_4$S$_8$ *Sci. Adv.* **1** 1500916

[18] Geng W R, Tang Y L, Zhu Y L, Wang Y J and Ma X L 2020 Boundary conditions control of topological polar nanodomains in epitaxial BiFeO$_3$(110) multilayered films *J. Appl. Phys.* **128** 184103

[19] Devonshire A F 1949 Theory of barium titanate *Philos. Mag.* **40** 1040
Devonshire A F 1951 Theory of barium titanate-Part II *Philos. Mag.* **42** 1065

[20] Landau L D and Lifshitz E M 1959 *Statistical Physics* (Oxford: Pergamon)

[21] Ginzburg V L 2001 Phase transitions in ferroelctrics: some historical remarks *Phys.-Usp.* **44** 1037 and reference therein

[22] Levanyuk A P, Misirlioglu I B and Okatan M B 2020 Landau, Ginzburg, Devonshire and others *Ferroelectrics* **569** 310

[23] Zhang C, Tewari S, Toner J and Das Sarma S 2008 Ginzburg-Landau theory for the conical cycloid state in multiferroics: applications to CoCr$_2$O$_4$ *Phys. Rev. B* **78** 144426

[24] Artyukhin S, Delaney K T, Spaldin N A and Mostovoy M 2014 Landau theory of topological defects in multiferroic hexangonal manganites *Nat. Mater.* **13** 42

[25] Ginzburg V L and Landau L D 1950 *JETP* **20** 1064

[26] Mostovoy M 2006 Ferroelectricity in spiral magnets *Phys. Rev. Lett.* **96** 067601

[27] Tokura Y and Seki S 2010 Multiferroics with spiral spin orders *Adv. Mater.* **22** 1554

[28] Li Y Q, Liu Y H and Zhou Y 2011 General spin order theory via gauge Landau-Lifshitz equation *Phys. Rev. B* **84** 205123

[29] Jin P Q, Li Y Q and Zhang F C 2006 SU(2)×U(1) unified theory for charge, orbit and spin currents *J. Phys. A: Math. Gen.* **39** 7115

[30] Ruseckas J, Juzeliunas G, Ohberg P and Fleischhauer M 2005 Non-Abelian gauge potentials for ultracold atoms with degenerate dark states *Phys. Rev. Lett.* **95** 010404

[31] Lu L H and Li Y Q 2007 The effects of optically induced non-Abelian gauge field in cold atoms *Phys. Rev. A* **76** 023410

[32] Landau L D and Lifshitz E M 1984 *Electrodynamics of Continuous Medias* (Oxford: Pergamon)

[33] King-Smith R D and Vanderbilt D 1993 Theory of polarization of crystalline solids *Phys. Rev. B* **47** 1651–4

[34] Essin A M, Moore J E and Vanderbilt D 2009 Magnetoelectric polarizability and axion electrodynamics in crystalline insulators *Phys. Rev. Lett.* **102** 146805

[35] Gilmore R 2005 *Lie Groups, Lie Algebras and Some of Their Applications* (New York: Dover)

[36] Yang C N and Mills R L 1954 Conservation of isotopic spin and isotopic invariance *Phys. Rev.* **96** 191

[37] Wilkens W 1994 Quantum phase of a moving dipole *Phys. Rev. Lett.* **72** 5

[38] Spaldin N A and Ramesh R 2019 Advances in magnetoelectric multiferroics *Nat. Mater.* **18** 203

[39] Tokura Y 2006 Multiferroics as quantum electromagnets *Science* **312** 1481

[40] Eerenstein W, Mathur N D and Scott J F 2006 Multiferroic and magnetoelectric materials *Nature* **442** 759

[41] Fiebig M, Lottermoser T, Meier D and Trassin M 2016 The evolution of multiferroics *Nature Rev. Mater.* **1** 1

[42] Kimura T, Goto T, Shintani H, Ishizaka K, Arima T and Tokura Y 2003 Magnetic control of ferroelectric polarization *Nature* **426** 55

[43] Lawes G *et al* 2005 Magnetically driven ferroelectric order in Ni$_3$V$_2$O$_8$ *Phys. Rev. Lett.* **95** 087205

[44] Kida N, Ikebe Y, Takahashi Y, He J P, Kaneko Y, Yamasaki Y, Shimano R, Arima T, Nagaosa N and Tokura Y 2008 Electrically driven spin excitation in the ferroelectric magnet DyMnO$_3$ *Phys. Rev. B* **78** 104414

[45] Fröhlich J and Studer U M 1993 Gauge invariance and current algebra in nonrelativistic many-body theory *Rev. Mod. Phys.* **65** 0034

[46] Leurs B W A, Zazario Z, Santiago D I and Zaanen J 2008 Non-Abelian hydrodynamics and the flow of spin in spin-orbital coupled substances *Ann. Phys.* **323** 907

[47] Tokura Y, Seki S and Nagaosa N 2014 Multiferroics of spin origin *Rep. Prog. Phys.* **77** 076501

[48] Faddeev L and Niemi A 2002 Aspects of electric and magnetic variables in SU(2) Yang-Mills theory *Phys. Lett. B* **525** 195

[49] Piette B M A G, Schores B J and Zakrzewski W J 1995 Dynamics of baby skyrmions *Nucl. Phys. B* **439** 205